Pis'ma v ZhETF, vol. 100, iss. 12, pp. 946 – 958

ПО ИТОГАМ ПРОЕКТОВ
РОССИЙСКОГО ФОНДА ФУНДАМЕНТАЛЬНЫХ ИССЛЕДОВАНИЙ
Проекты РФФИ # 11-02-00146а

High-temperature Aharonov–Bohm effect in transport through a single-channel quantum ring[1)]

A. P. Dmitriev[+*], *I. V. Gornyi*[+*], *V. Yu. Kachorovskii*[+*2)], *D. G. Polyakov*[*], *P. M. Shmakov*[+]

[+]*Ioffe Physico-Technical Institute of the RAS, 194021 St. Petersburg, Russia*

[*]*Institut für Nanotechnologie, Karlsruhe Institute of Technology, 76021 Karlsruhe, Germany*

Submitted 5 November 2014

We overview transport properties of an Aharonov–Bohm interferometer made of a single-channel quantum ring. Remarkably, in this setup, essentially quantum effects survive thermal averaging: the high-temperature tunneling conductance G of a ring shows sharp dips (antiresonances) as a function of magnetic flux. We discuss effects of electron-electron interaction, disorder, and spin-orbit coupling on the Aharonov–Bohm transport through the ring. The interaction splits the dip into series of dips broadened by dephasing. The physics behind this behavior is the persistent-current-blockade: the current through the ring is blocked by the circular current inside the ring. Dephasing is then dominated by tunneling-induced fluctuations of the circular current. The short-range disorder broadens antiresonances, while the long-range one induces additional dips. In the presence of a spin-orbit coupling, G exhibits two types of sharp antiresonances: Aharonov–Bohm and Aharonov-Casher ones. In the vicinity of the antiresonances, the tunneling electrons acquire spin polarization, so that the ring serves as a spin polarizer.

DOI: 10.7868/S0370274X14240163

1. Introduction. A major focus of interest in nanophysics [1] has been quantum interference effects on one hand and charge-quantization effects on the other, both of which become more prominent with decreasing dimensionality and size of the device. The prime device for specifically probing the interference of electrons is a quantum ring connected to the leads. The conductance of the ring $G(\phi)$ exhibits the Aharonov–Bohm (AB) effect [2, 3], i.e., changes periodically with the dimensionless magnetic flux $\phi = \Phi/\Phi_0$ threading the ring – with a period 1 – entirely due to the interference of electron trajectories winding around the hole (here $\Phi_0 = hc/e$ is the flux quantum). This effect is one of the most beautiful manifestations of the wave nature of electrons. The key physical issue – the sensitivity of the phase of an electronic wavefunction to a magnetic flux – enables the design of quantum AB interferometers [4–20] that can be tuned by an external magnetic field.

The simplest realization of such an interferometer is a *single-channel* electronic quantum ring with a *tunneling coupling* to the leads, Fig. 1. Direct confrontation with experiment appears now to be possible since many-electron nanorings with a few or single conducting channels have been manufactured [21–25]. In this paper, we overview transport properties of this archetypic setup and demonstrate that they are governed by quantum effects even at high temperatures.

At low temperature T, the tunneling conductance of this device exhibits narrow resonant peaks [26–33]. The peak arises each time when one of the flux-dependent energy levels in the ring crosses the Fermi energy (AB resonances are also affected by the Coulomb blockade [34, 35]). Based on this physical picture, one could expect the suppression of the resonance structure at $T \gg \gg \Delta$, where Δ is the level spacing in the ring. Remarkably, this naive expectation is incorrect and the interference effects are not entirely suppressed by the thermal averaging. In particular, for $T \gg \Delta$ the conductance of the noninteracting clean ring tunnel-coupled to the contacts exhibits sharp narrow dips (antiresonances) at

[1)]See Supplemental material for this paper on JETP Letters suite: www.jetpletters.ac.ru.

[2)]e-mail: kachor.valentin@gmail.com

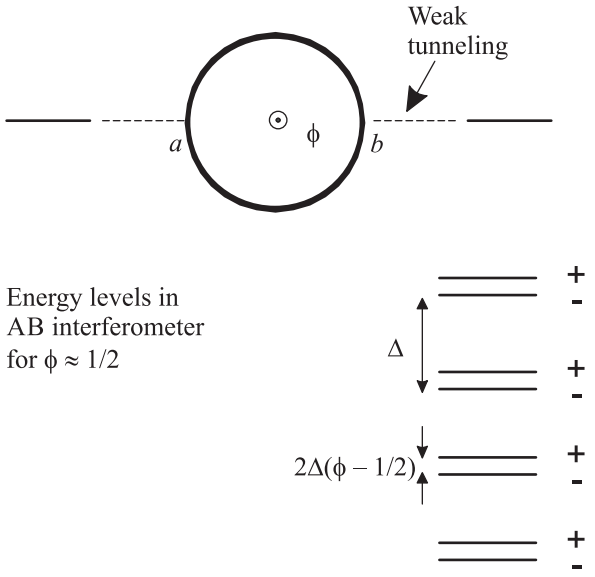

Fig. 1. Single-channel quantum ring and its energy levels

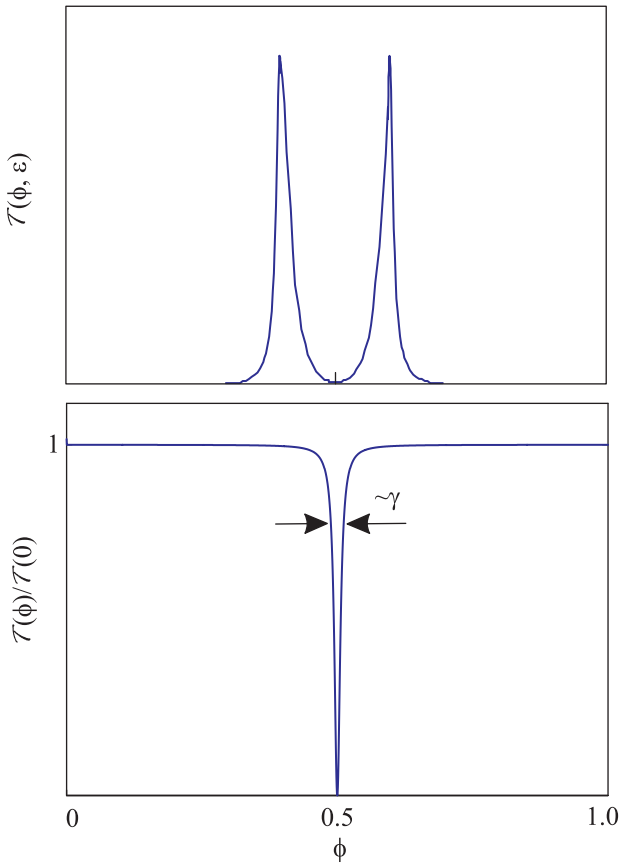

Fig. 2. Resonances in the transmission coefficient of a clean non-interacting ring at given energy (upper panel) and antiresonance in the thermally-averaged transmission coefficient (lower panel)

$\phi = 1/2 + n$, where n is integer (see Fig. 2) [36–38]. The physics behind this antiresonance is the destructive interference in the tunneling process via pairs of quantum levels in the ring. For $\phi = 1/2$ the levels with opposite parities are exactly degenerate. On the other hand, the tunneling amplitudes for such levels have opposite signs, so that the total transmission coefficient is exactly zero for an arbitrary energy ϵ of the tunneling electron: $\mathcal{T}(\phi, \epsilon)|_{\phi=1/2} \equiv 0$. As a consequence, the averaged transmission coefficient $\mathcal{T}(\phi) = \langle \mathcal{T}(\phi, \epsilon) \rangle_\epsilon$ (here averaging is taken over temperature window) shows a sharp antiresonance (see Fig. 2). This effect and its generalizations in the presence of electron-electron interaction, disorder, and spin-orbit (SO) coupling is the subject of this review.

The basic physics of the single-channel AB interferometer made up of – ultimately one-dimensional (1D) – quantum wires becomes conceptually intricate in the presence of interaction. Indeed, it is well known that $e-e$ interactions in 1D transform the electron gas into a Luttinger liquid (LL) [39]. A key concept in the study of coherent transport of interacting electrons is that of dephasing of electron waves, which at low temperature T is due to electromagnetic fluctuations produced by $e-e$ interactions [1]. The AB effect is one of the most convenient tools for studying the dephasing processes, since these directly govern the amplitude of the flux-dependent part of $G(\Phi)$. The distinguishing property of a single-channel AB interferometer in the tunneling regime is that the dephasing rate is dramatically suppressed due to the quantization in an almost closed ring [38]. The interference pattern in the presence of interaction consists of a series of antiresonances broadened by dephasing. The physics behind this behavior is the persistent-current-blockade: the current through the ring is blocked by the circular current inside the ring. Dephasing is then dominated by tunneling-induced fluctuations of the (almost quantized) circular current.

The effect of disorder on the high-temperature transport through a quantum ring depends on the range of impurity potential [40]. In the absence of electron-electron interaction, the short-range potential broadens the AB antiresonances, while the long-range smooth disorder induces negative resonant peaks at integer values of the flux. The shape of the peaks in the presence of disorder turns out to be essentially non-Lorentzian.

The spin-dependent transport through a ballistic single-channel AB interferometer in the presence of spin-orbit coupling exhibits the interplay of AB and Aharonov–Casher (AC) effects [41]. Importantly, the spin-selective properties of the quantum-ring setup also survive the thermal averaging. Specifically, the SO in-

teraction leads to the splitting of the high-temperature conductance antiresonances into two dips, the distance between dips being proportional to the AC phase. The latter is the spin analog of the orbital AB phase and arises due to a built-in effective magnetic field induced by the SO coupling. In the vicinities of the dips the tunneling electrons acquire polarization $\mathbf{P}(\phi)$. At zero external field ($\phi = 0$) the conductance $G(0)$ exhibits series of sharp AC antiresonances.

The review is organized as follows. In Section 2 we discuss the transmission through a clean ring without interactions. Section 3 overviews the physics in a clean ring with the electron-electron interaction. Section 4 is focused on the disordered non-interacting ring. Finally, the setup with a SO coupling is discussed in Section 5. In all the cases, we address the high-temperature regime,

$$T \gg \Delta \gg \Gamma, \tag{1}$$

where Γ is the tunneling rate.

2. Clean quantum ring: noninteracting electrons. The conductance of a ring $G(\phi) = G(\phi + 1)$ is a periodic function of ϕ irrespective of the particular form of the electron Hamiltonian. We begin by discussing the behavior of $G(\phi)$ for $T \gg \Delta$ in the case of a clean (disorder-free) ring and noninteracting electrons. For elastic transmission, $G(\phi)$ per spin in units of e^2/h is given, in the linear response limit, by the thermally-averaged transmission coefficient:

$$G(\phi) = \mathcal{T}(\phi) \equiv \langle \mathcal{T}(\phi, \epsilon) \rangle_\epsilon, \tag{2}$$

where $\langle \ldots \rangle_\epsilon = -\int d\epsilon \, (\ldots) \partial_\epsilon f_T$ and $f_T(\epsilon)$ is the Fermi distribution. Below, we neglect the ϵ dependence of the envelope of the otherwise periodic-in-ϵ, with a period Δ, function $\mathcal{T}(\phi, \epsilon)$ in the vicinity of the Fermi energy ϵ_F for $|\epsilon - \epsilon_\mathrm{F}| \lesssim T$. Then, Eq. (2) in the limit $T \gg \Delta$ reduces to the average over ϵ within the interval of width Δ. For the linearized dispersion relation with velocity v, the Hamiltonian of noninteracting electrons in an isolated ring in the presence of flux ϕ is written as $H_\mathrm{ring} = -iv \sum_\mu \int_0^L dx \, \psi_\mu^\dagger (\partial_x - 2\pi i \phi / L) \psi_\mu$, where $\mu = \pm$ is the electron chirality, L the circumference of the ring.

Consider first a fully symmetric setup, with identical tunnel contacts and the interferometer arms of equal length (Fig. 1). Assume also that the tunnel contacts are pointlike, with the tunnel Hamiltonian given by

$$H_\mathrm{tun} = t_0 [\, \psi_L^\dagger \psi(0) + \psi_R^\dagger \psi(L/2) + \mathrm{h.c.}], \tag{3}$$

where ψ_L (ψ_R) are the electron operators in the left (right) lead (not necessarily a one-dimensional lead) at the points of the contacts and $\psi(x) = \psi_+(x) + \psi_-(x)$. The tunneling rate (in the limit of weak tunneling) reads $\Gamma = 2\gamma\Delta/\pi$, where $\Delta = 2\pi v/L$ is the level spacing in the isolated ring for given chirality and the dimensionless parameter $\gamma = (2\pi\rho/v)|t_0|^2$ (tunneling transparency of the contact) is expressed in terms of ρ, the (assumed structureless) density of states in the leads at the points of the contacts.

In the tunnel-coupled ring, electrons experience backscattering at the contacts, the amplitude of which (for real t_0) is $t_b = -\gamma/(1+\gamma)$. The amplitude to stay in the ring without changing chirality after passing the contact reads $t_{in} = 1/(1+\gamma)$. The amplitude of transmission through the ring $t(\phi, \epsilon)$ is given by a sum of the amplitudes of the trajectories that connect contact a to contact b (Fig. 1), including those with multiple backscattering by the contacts [38, 40]:

$$t(\phi, \epsilon) = \sum_{n=0}^{\infty} (\beta_n^- + \beta_n^+) e^{ikL(n+1/2)}, \tag{4}$$

where n is the number of times the electron passes contact b without exiting the ring and k is the wavenumber. All trajectories for given n, with an arbitrary sequence of chiralities, have the same length $L(n + 1/2)$. The terms β_n^- and β_n^+ separate the contributions of trajectories that end up running clock- and counterclockwise, respectively. These satisfy the recursion relation

$$\boldsymbol{\beta}_{n+1} = \hat{A} \boldsymbol{\beta}_n \tag{5}$$

for the vector $\boldsymbol{\beta}_n = (\beta_n^+, \beta_n^-)$, where

$$\hat{A} = \begin{bmatrix} t_{in}^2 e^{-2\pi i \phi} + t_b^2 & t_b t_{in} (e^{-2\pi i \phi} + 1) \\ t_b t_{in} (e^{2\pi i \phi} + 1) & t_{in}^2 e^{2\pi i \phi} + t_b^2 \end{bmatrix}. \tag{6}$$

The element A_{ij} of the matrix $\hat{A}$ (multiplied by $\exp(ikL)$) is the sum of the amplitudes of the trajectories starting at the contact b (see Fig. 1) and making a single return to the same contact (indices i and j specify, respectively, the final and initial directions of motion: $i = \pm, j = \pm$). The components of the vector $\boldsymbol{\beta}_0$: $\beta_0^\pm = -2\gamma e^{\mp i\pi\phi}/(1+\gamma)^2$, yield contributions of shortest counterclockwise and clockwise trajectories, respectively. Importantly, at $\phi = 1/2$, for each path contributing to β_n^- there exists a "mirrored" path (with $\mu \to -\mu$ on each segment) whose contribution to β_n^+ has an opposite sign. It is this destructive interference that leads to the vanishing of $\mathcal{T}(1/2, \epsilon)$ for arbitrary ϵ (and, therefore, to the vanishing of $G(1/2)$ in the case of noninteracting electrons for any dispersion relation and any distribution function).

In the limit $T \gg \Delta$, only the products of amplitudes with the same n are not suppressed in $\langle|t(\phi,\epsilon)|^2\rangle_\epsilon$ by thermal averaging, so that, for the ϵ-independent $\beta_n^\pm$,

$$\mathcal{T}(\phi) = \sum_{n=0}^{\infty} |\beta_n^- + \beta_n^+|^2 = \sum_{n=0}^{\infty} \left|(\mathbf{e}\cdot\hat{A}^n\boldsymbol{\beta}_0)\right|^2, \qquad (7)$$

where $\mathbf{e} = (1,1)$ is the unit vector. The sum in Eq. (7) is expressible [40], quite generally, solely in terms of $\det\hat{A}$ and $\mathrm{Tr}\hat{A}$. For $\hat{A}$ from Eq. (6), the result reads [38, 40]

$$\mathcal{T}(\phi) = \frac{2\gamma\cos^2(\pi\phi)}{\cos^2(\pi\phi)+\gamma^2}. \qquad (8)$$

For $\gamma \ll 1$, the antiresonance has a Lorentzian shape:

$$\mathcal{T}(\phi) \simeq 2\gamma\frac{\pi^2(\delta\phi)^2}{\pi^2(\delta\phi)^2+\gamma^2}\ , \qquad (9)$$

where $\delta\phi = \phi - 1/2$ (Fig. 2).

Apart from the cancellation of the contributions of mirrored paths in Eq. (4), the Lorentzian in Eq. (9) can be understood [38, 40] as following from the destructive interference in resonant scattering on pairs of almost degenerate (for $|\delta\phi| \ll 1$) levels of different "parity". In a closed ring, the energies of states with chirality μ are given by $\epsilon_m^\mu = (m-\mu\phi)\Delta$, where m is an integer. The eigenfunctions are the circulating waves $\psi_m^\pm(x) \propto \exp(\pm 2\pi i m x/L)$. At $\phi = 1/2$, all the levels are exactly double degenerate with $\epsilon_{m+1}^+ = \epsilon_m^-$ (this is true, in fact, for an arbitrary dispersion law). In the vicinity of the level crossing (Fig. 1), resonant scattering on the level pairs yields

$$\mathcal{T}(\phi) \simeq 4\gamma^2 v^2 \left\langle \left|\sum\nolimits_m g_m(\epsilon, L/2)\right|^2 \right\rangle_\epsilon , \qquad (10)$$

where

$$g_m(\epsilon,x) = \frac{1}{L}\left[\frac{e^{2i\pi(m+1)x/L}}{\epsilon-\epsilon_{m+1}^+ + i\Gamma/2} + \frac{e^{-2i\pi mx/L}}{\epsilon-\epsilon_m^- + i\Gamma/2}\right] \qquad (11)$$

is the contribution of the mth two-level system to the electron Green function inside the ring, with the resonant escape of electrons into the leads accounted for (solely) by the broadening in the energy denominators [40]. The two terms in $g_m(\epsilon, L/2)$ exactly cancel each other for $\phi = 1/2$. In the limit $\gamma \ll 1$, the integrand $|\sum_m g_m|^2$ in Eq. (10) reduces to the sum over the pairs $\sum_m |g_m|^2$. In turn, $|g_m|^2$ can be represented as a sum of the "classical" contribution, which describes independent scattering on each of the levels in the pair, and the interference contribution, which comes from the product of two terms in g_m. The corresponding classical contribution to the conductance, $\mathcal{T}_{\rm cl}(\phi) = 2\gamma$, is ϕ independent, whereas the interference contribution, $\mathcal{T}_{\rm int}(\phi) = -2\gamma^3/[\gamma^2 + \pi^2(\delta\phi)^2]$, is sharply peaked at $\phi = 1/2$. The sum $\mathcal{T}(\phi) = \mathcal{T}_{\rm cl}(\phi) + \mathcal{T}_{\rm int}(\phi)$ reproduces the Lorentzian in Eq. (9).

Note that, in the isolated ring, all energy levels are double degenerate at both half-integer and integer fluxes (in the latter case, with $\epsilon_m^+ = \epsilon_m^-$). However, resonant scattering on the pairs of levels of the same parity does not lead to any resonant feature in $\mathcal{T}(\phi)$ in Eq. (8) at $\phi = 0$. This is because of multiple backscattering at the contacts (inside the ring) that crucially affects resonant scattering at $\phi = 0$ [38], in contrast to $\phi = 1/2$. At $|\phi| \lesssim \gamma$, even if the amplitude of a single backscattering event is small ($\gamma \ll 1$), the enhancement of the effect of backscattering by multiple returns totally suppresses the resonance at the level (anti)crossing (at order $\mathcal{O}(\gamma)$, the vanishing of the resonance at $\phi = 0$ has been shown by directly summing up the return amplitudes in Ref. [38]).

Now let us turn to an asymmetric interferometer with the arm lengths $(L \pm a)/2$. The transmission coefficient for $T \gg \Delta$ and the length mismatch $a \ll L$ reads (see Appendix in the arXiv version of Ref. [38] at arXiv:0911.0911):

$$\mathcal{T}(\phi) = 2\gamma\left\langle \frac{\cos^2(\pi\phi)\cos^2(ka/2)}{\cos^2(\pi\phi)+\gamma^2\cos^2(ka/2)} + (\cos\to\sin)\right\rangle_\epsilon , \qquad (12)$$

where in the second term the cosines from the first term are changed to the sines of the same argument. In the limit $Ta/v \gg 1$, thermal averaging in Eq. (12) reduces to averaging over the phase ka within the interval of width 2π, which gives

$$\mathcal{T}(\phi) = 2\gamma\,[\,F(\cos\pi\phi) + F(\sin\pi\phi)\,], \qquad (13)$$

where $F(z) = z^2\left[\sqrt{z^2+\gamma^2}\left(|z| + \sqrt{z^2+\gamma^2}\right)\right]^{-1}$. For $\gamma \ll 1$, the function $G(\phi)$ in Eq. (13) shows sharp antiresonances at both half-integer and integer ϕ. In contrast to Eq. (8), however, $G(\phi)$ does not vanish at the resonance points, with the depth of the antiresonances at both $\phi = 0$ and $1/2$ being half that of the antiresonance at $\phi = 1/2$ for $a = 0$. Thus, in the strongly asymmetric setup with $Ta/v \gg 1$, the amplitude of the dips at half-integer fluxes becomes smaller compared to the symmetric case, while the additional dips appear at integer fluxes. The shape of the dips, even for $\gamma \ll 1$, is now more complicated than the Lorentzian (cf. Eq. (9)):

$$\mathcal{T}(\phi) \simeq \gamma + \frac{2\gamma\pi^2(\delta\phi)^2}{\sqrt{\pi^2(\delta\phi)^2+\gamma^2}\left[\pi|\delta\phi| + \sqrt{\pi^2(\delta\phi)^2+\gamma^2}\right]}, \qquad (14)$$

where $\delta\phi$ is the deviation from the resonance.

In the opposite limit of $Ta/v \ll 1$, the averaging over ϵ in Eq. (12) amounts to substituting the Fermi wavevector k_F for k. For $\gamma \ll 1$, there are then two series of narrow antiresonances, at integer and half-integer fluxes. Unlike in Eq. (13), the series are not simply shifted in ϕ by half a period. For the antiresonance at an integer flux,

$$\mathcal{T}(\phi) \simeq 2\gamma \left[\cos^2(k_F a/2) + \frac{\pi^2(\delta\phi)^2 \sin^2(k_F a/2)}{\pi^2(\delta\phi)^2 + \gamma^2 \sin^2(k_F a/2)}\right], \tag{15}$$

whereas $\mathcal{T}(\phi)$ around a half-integer flux is given by Eq. (15) with the change $\cos(k_F a/2) \leftrightarrow \sin(k_F a/2)$. The amplitudes and the widths of the dips are seen to oscillate with varying $k_F a$. In Fig. 3, the dependence of $\mathcal{T}$ on ϕ for $\Delta \ll T \ll v/a$ is shown for $k_F a = 2\pi/3$.

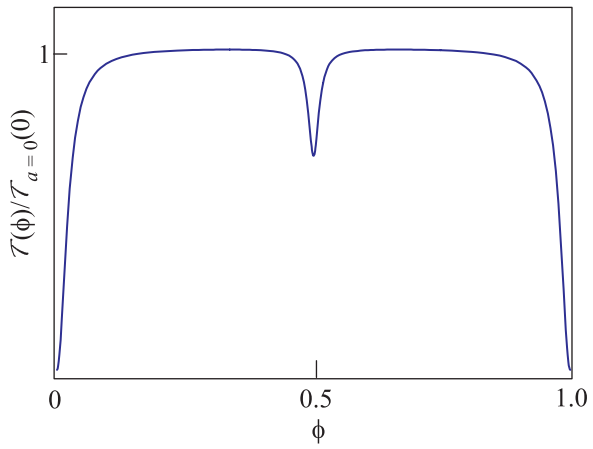

Fig. 3. Conductance G vs flux ϕ for $k_F a = 2\pi/3$. The tunneling parameter $\gamma = 0.08$

3. Clean interacting ring. The inclusion of electron-electron interactions leads to profound changes in the behavior of $G(\phi)$ (which is no longer equals to single-particle transition coefficient $\mathcal{T}(\phi)$), as summarized in Fig. 4. As the strength of interaction α increases, the single antiresonance at $\phi = 1/2$ (Fig. 4a) first becomes shallower and broader (Fig. 4b) and then splits up into a series of sharp antiresonances (Fig. 4c) that show up all the way between $\phi = 0$ and 1. These interaction-induced oscillations, termed in Ref. [38] "persistent-current blockade" (PCB), are due to a peculiar type of interaction of electrons with the *circular* current J inside the ring, resulting in the blocking, for specific values of ϕ, of the *tunneling* current through the ring. In essence, the interaction with the current J (quantized due to charge quantization) amounts to the addition of an effective magnetic flux acting on electrons,

$$\delta\phi_J = -\alpha J/2, \tag{16}$$

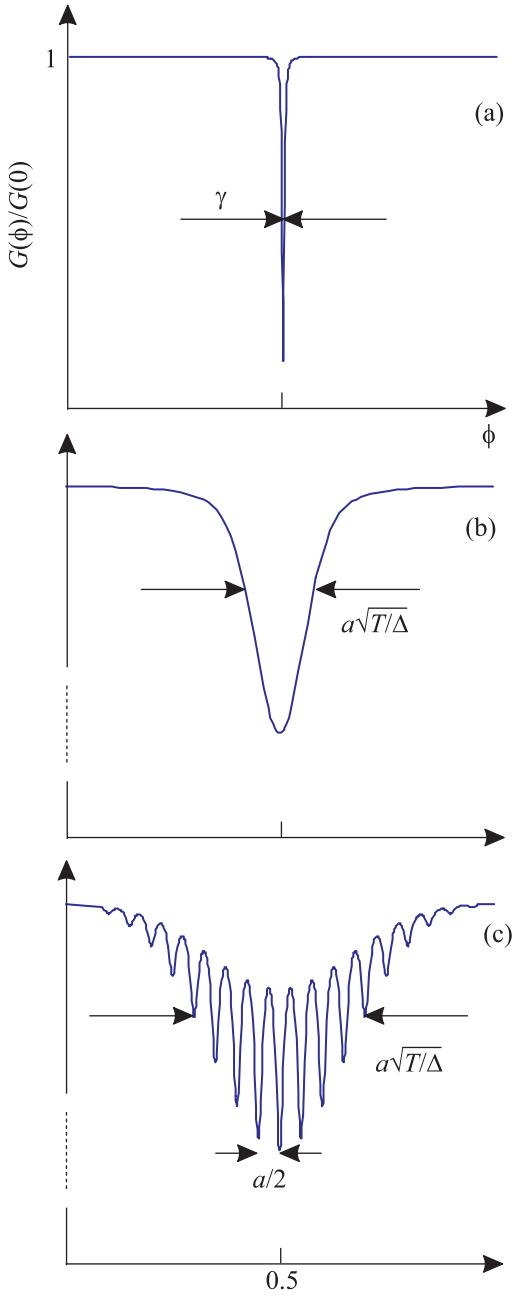

Fig. 4. Schematic evolution of $G(\Phi)$ with increasing interaction strength α: $\alpha \ll (\Gamma^2/\Delta T)^{1/2}$: a single narrow deep antiresonance at $\phi = 1/2$ (a); $(\Gamma^2/\Delta T)^{1/2} \ll \alpha \ll \Gamma T/\Delta^2$: the antiresonance broadens and becomes shallower (b); $\alpha \gg \Gamma T/\Delta^2$: breaking up of the antiresonance into "persistent-current blockade" oscillations (c). For fixed α, the evolution with increasing T follows (a) $\to$ (c) $\to$ (b)

which produces a shift of the total flux (note that the effective flux produced by the circulating current is not at all related to the relativistic Biot–Savart law).

The PCB oscillations – in contrast to the Coulomb-blockade oscillations [1] – survive thermal averaging at

large T but are suppressed by dephasing. In a tunnel-coupled ring, the persistent current exhibits thermal fluctuations, because of exchange of electrons between the ring and the leads, accompanied by fluctuations of the effective flux. These fluctuations are the main source of dephasing of the AB oscillations, with the dephasing rate given by

$$\gamma_\varphi = 4\Gamma T/\Delta. \tag{17}$$

This "zero-mode dephasing" (ZMD) is strongly affected by quantization of charge inside the ring: γ_φ vanishes at $\Gamma \to 0$. Being peculiar to closed geometry, ZMD is qualitatively different from dephasing in open geometry, where two quantum wires with a magnetic flux between them are weakly tunnel-coupled at two points. In the latter case, the dephasing rate is given by the single-particle decay rate in a homogeneous Luttinger liquid ($\sim \alpha^2 T$ for spinless electrons) [42–46]. A remarkable feature of γ_φ in Eq. (17) is that it does not depend on α[3)].

We assume that the Coulomb interaction is screened by a ground plane and take the interaction to be point-like. The interacting part of the Hamiltonian reads

$$H_{\rm int} = \frac{V_0}{2}\sum_\mu \int_0^L dx\, n_\mu n_{-\mu}, \tag{18}$$

with the dimensionless interaction constant $\alpha = V_0/2\pi v$. In this section, we focus on the case of spinless electrons. The repulsion between electrons with the same μ is then accounted for completely in the renormalization of the velocity v [45, 46]. The velocity of single-particle excitations is further renormalized by the interaction between oppositely moving electrons and becomes equal to the plasmon velocity $u = v(1-\alpha^2)^{1/2}$ (the renormalized level spacing is $\Delta = 2\pi u/L$).

The renormalization of the triple junctions a and b due to virtual processes on energy scales larger than T yields a T dependent tunneling rate $\Gamma(T)$ [47]. In particular, for $\alpha \gg \Gamma/\Delta$, backscattering inside the ring at the tunnel contact may be neglected in the renormalization process and $\Gamma(T) \sim \Gamma(\epsilon_{\rm F}/T)^{(1-K)^2/2K}$, where $K = (1-\alpha)^{1/2}(1+\alpha)^{-1/2}$ is the Luttinger constant. For $T \gg \Delta$, two contacts are renormalized independently.

3.1. Persistent-current blockade. For $T \gg \Delta$, the effect of electron-electron interactions on the single- particle transmission amplitudes can be described in terms of scattering on the thermal electromagnetic noise created by the bath of other electrons. Consider first the bath with the total number N_μ of electrons in the channel μ being a quantum number. For the linear dispersion relation, the density profile $n_\mu(x)$ for a given chirality remains unchanged at $\Gamma = 0$ and rotates as a whole. The forward scattering of electrons of chirality μ is then fully accounted for through the phase they acquire in the time-dependent potential $U_\mu(x,t) = V_0 n_{-\mu}(x+\mu u t)$. The quasiclassical amplitude of the transition from $x = 0$ to $L/2$ without winding around the hole is then given by $\mathcal{A}_1^\mu = \exp\left\{i\pi\mu\phi + iV_0\int_0^{L/2u} dt\, n_{-\mu}[x(t)+\mu u t]\right\}$. A crucial point is that, even though the time integration is taken over the *half*-period, for $x(t) = \mu u t$ the integral is insensitive to a particular profile of $n_{-\mu}$ and only depends on $N_{-\mu}$. This holds true also for the amplitude with an arbitrary winding number n. As a result, the interference term in the conductance,

$$\mathcal{A}_k^+ \bar{\mathcal{A}}_k^- = \exp\{2\pi i k[\phi - \alpha(N_+ - N_-)/2]\}, \tag{19}$$

is not suppressed by thermal averaging over fluctuations of $n_\pm(x,t)$ at fixed $N_\pm$ (it is this averaging that is responsible for the exponential decay of single-particle excitations in an infinite Luttinger liquid). That is, plasmons in the isolated ring do not lead to any dephasing.

Thus, apart from the renormalization of Γ and Δ, the only effect of the interaction with the bath characterized by fixed N_μ is the effective shift of the flux given by Eq. (16) with $J = N_+ - N_-$. Note that the phase shift (16) between two interfering waves stems from the absence of electron-electron scattering within the same channel μ (Hartree–Fock cancellation [45, 46]). In effect, for given J, electrons of opposite chirality see different electrostatic potentials, which translates into the phase difference in Eq. (19). Being inserted in Eq. (8), $\delta\phi_J$ yields a shift of the AB antiresonance, i.e., the PCB completely blocks the tunneling current through the ring at $\phi = 1/2 - \delta\phi_J$.

For a thermodynamic ensemble of the "isolated baths", the conductance should be averaged over the Gibbs distribution of the zero-mode energies [48],

$$\epsilon_{N_+N_-} = (\Delta/4K)\left[(N-N_0)^2 + K^2(J-2\phi)^2\right], \tag{20}$$

where N_0 is controlled by the chemical potential and $N = N_+ + N_-$ is the total number of electrons in the ring. Equation (20) describes, quite generally, electrostatics of a 1D ring. The resulting conductance as a function of ϕ shows PCB oscillations with a period $\alpha/2$ and a Gaussian envelope whose width $w_T = \alpha(T/\Delta)^{1/2}$ is entirely determined by the statistical weights of different values of J.

3.2. Zero-mode dephasing. Taking into account the ergodic tunneling dynamics of the electron bath, i.e., the

[3)] More accurately, α enters in the renormalization of Γ and the condition of the applicability of Eq. (17) $\alpha \gg \Gamma/\Delta$.

time dependence of the circular current, leads to PCB oscillations in a *single* ring. In contrast to the isolated ring, each PCB resonance acquires a width induced by a finite lifetime of the state with given J. Importantly, this time is much shorter than the single-electron tunneling lifetime Γ^{-1}. Indeed, the time scale for changing J by unity is given by Γ^{-1} divided by the number of levels T/Δ around the Fermi level that participate in the tunneling dynamics. We identify the interaction-induced broadening of the PCB resonances with dephasing (Eq. (17)).

For a quantitative analysis of $G(\phi)$, we average the product of the amplitudes in Eq. (19) over realizations of $J(t)$. This gives the interaction-induced action $S(t_n)$, where $t_n = 2\pi(n+1/2)/\Delta$ for the winding number n:

$$e^{-S(t)} = \left\langle \exp\left\{-i\alpha\Delta\int_0^t dt'[N_+(t') - N_-(t')]\right\}\right\rangle .$$

The interference term $\delta G(\phi) = G(\phi) - G(0)$ is affected by this action:

$$\frac{\delta G(\phi)}{G(0)} \simeq -\frac{2\pi\Gamma}{\Delta}\sum_{n=0}^{\infty}\cos(2\Delta\delta\phi t_n)\, e^{-\Gamma t_n - S(t_n)}. \quad (21)$$

Next, we represent $N_\mu = \sum_j n_j^\mu$ as a sum over individual energy levels inside the ring. Due to the slow tunneling exchange with the lead, the occupation numbers n_j^μ fluctuates between two values, 0 and 1. Hence, the time evolution of these numbers is a telegraph noise with the rates Γf_j and $\Gamma(1-f_j)$ for scattering "in" (population rate of an empty level with $n_j^\mu = 0$) and "out" (depopulation rate of an occupied level with $n_j^\mu = 1$), respectively. Here f_j is the distribution function at the energy of the jth level. This function is the same for energy levels in the ring and in the lead. The phase factor induced by the interaction with the jth level is written as (we suppress the indexes j and μ for brevity)[4)]:

$$\left\langle e^{-i\alpha\Delta\int_0^t dt'\, n(t')}\right\rangle = (1-f)\,(P_{00}+P_{01}) + f\,(P_{10}+P_{11}),$$

where $P_{kl}(t)$ is the conditional quasiprobability, which yields the mathematical expectation of the phase factor $\exp[-i\alpha\Delta\int_0^t dt'\, n(t')]$ under the condition that the initial and final electron states have the occupation numbers k and l, respectively. The quasiprobabilities satisfy the master equations

$$dP_{00}/dt = -\Gamma f P_{00} + \Gamma(1-f)P_{01}, \quad (22)$$

$$dP_{01}/dt = \Gamma f P_{00} - [i\alpha\Delta + \Gamma(1-f)]P_{01}, \quad (23)$$

$$dP_{10}/dt = -\Gamma f P_{10} + \Gamma(1-f)P_{11}, \quad (24)$$

$$dP_{11}/dt = \Gamma f P_{10} - [i\alpha\Delta + \Gamma(1-f)]P_{11}, \quad (25)$$

with the initial conditions $P_{00}(0) = P_{11}(0) = 1$, $P_{01}(0) = P_{01}(0) = 0$.

For closed ring ($\Gamma = 0$) we get $P_{00} = 1$, $P_{01} = P_{10} = 0$, $P_{11} = e^{i\alpha\Delta t}$, so that the averaged phase factor reads

$$\left\langle e^{-i\alpha\Delta\int_0^t dt'\, n(t')}\right\rangle_{\Gamma=0} = 1 - f + f e^{-i\alpha\Delta t},$$

and the action at $\Gamma = 0$ is given by

$$e^{-S_0(t)} = \prod_j |1 - f_j + f_j e^{-i\alpha\Delta t}|^2 \approx$$

$$\approx \exp\left[-\frac{2T}{\Delta}(1-\cos\alpha\Delta t)\right] \approx \exp\left[-\alpha^2 T\Delta\{t^2\}\right],$$

where $\{\ldots\}$ denotes a periodic continuation in t from the interval $-\pi/\alpha\Delta < t < \pi/\alpha\Delta$. One can check that Eq. (26) is nothing but the thermodynamic average $e^{-S_0(t)} = \left\langle e^{-i\alpha J\Delta t}\right\rangle_{\text{Gibbs}}$ over the zero-mode energies (20). We see that the function $e^{-S_0(t)}$ is sharply peaked at the points $t = 2\pi m/\alpha\Delta$ with integer $m \geq 0$ (see Fig. 5). Hence, in the closed ring the factor $e^{-S_0(t)}$

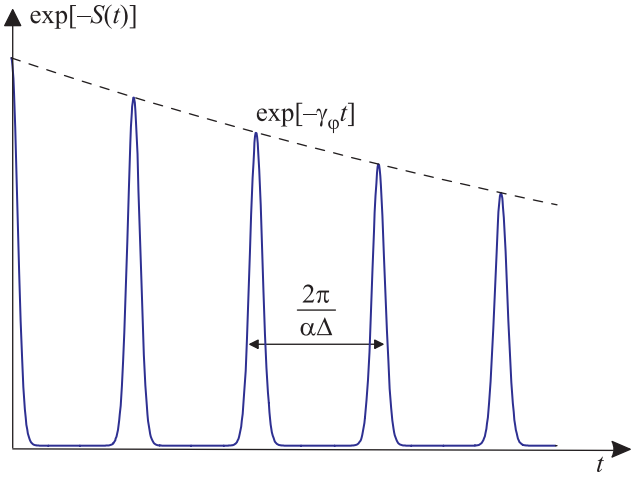

Fig. 5. Quantum beats in the dephasing action and slow dephasing

does not decay and shows sharp PCB resonances (quantum beats).

For $\Gamma \neq 0$, the solution of the master equations yields $S(t) = -2\mathrm{Re}\sum_j \ln\left[\left(e^{\lambda_j^+ t}\lambda_j^- - e^{\lambda_j^- t}\lambda_j^+\right)/\left(\lambda_j^- - \lambda_j^+\right)\right]$, where $\lambda_j^\pm = \lambda - i\alpha\Delta f_j \pm (\lambda^2 + i\alpha\Delta\Gamma f_j)^{1/2}$ and $\lambda = (i\alpha\Delta - \Gamma)/2$. For $\alpha \gg \Gamma/\Delta$, the sum in Eq. (21) is cut off by $S(t)$ at $t_n \ll \Gamma^{-1}$, so that we can expand $S(t)$ in Γ. The linear-in-Γ term,

$$S_1(t) \simeq \frac{4\Gamma T}{\Delta}\eta(t)\left[t\cos^2\left(\frac{\alpha\Delta t}{2}\right) - \frac{\sin(\alpha\Delta t)}{\alpha\Delta}\right], \quad (26)$$

with $\eta(t) = \alpha\Delta\{t\}/\sin(\alpha\Delta t)$ is responsible for the dephasing. For $\alpha \ll (\Delta/T)^{1/2}$, the sum in Eq. (21) can be

[4)] A similar approach was used to describe dephasing of a qubit by a two-level fluctuator, see Refs. [49–51] and references therein.

replaced by an integral. The latter is dominated by the vicinity of the points $t = 2\pi m/\alpha\Delta$. At these points for $m \gg 1$,

$$S_1(t) \simeq \gamma_\varphi t,$$

with the dephasing rate γ_φ given by Eq. (17). The dependence of dephasing action on time is schematically plotted in Fig. 5. From Eq. (21) we finally find that the interference term then can be cast in the form of a Gibbs sum over zero-mode states:

$$\frac{\delta G(\phi)}{G(0)} \simeq \left\langle \frac{\Gamma\gamma_\varphi}{(2\delta\phi - \alpha J)^2\Delta^2 + \gamma_\varphi^2} \right\rangle_{\text{Gibbs}} \simeq$$
$$\simeq \operatorname{Im} \frac{(\Gamma/2w_T\Delta)\exp(-\delta\phi^2/w_T^2)}{\sin[\,\pi(\delta\phi + 2i\gamma_\varphi/\Delta)/\alpha\,]}. \qquad (27)$$

If $\alpha\Delta \gg \gamma_\varphi$, Eq. (27) yields well- separated Lorentzians (Fig. 4c) of width γ_ϕ/Δ, centered at integer $\delta\phi/\alpha$. Note that, despite the appearance of the PCB fine structure, the exact period in ϕ remains unity, as it should be. In the opposite limit, $\alpha\Delta \ll \gamma_\varphi$, the broadening of the resonances is larger than the distance between them, so that they merge into a single Gaussian dip of width w_T (Fig. 4b). Equation (27) describes the physically most transparent case of not too large $\alpha \ll (\Delta/T)^{1/2}$, which means that the width w_T of the envelope of the PCB resonances is much smaller than the period of the AB oscillations. At larger α, additional features appear; in particular, related to a possible commensurability between $\delta\phi_J$ and 1 – these will be considered elsewhere.

It is worth noting that the tunneling broadens also the plasmon levels inside the ring, which introduces an additional contribution $\gamma_\varphi^{\text{p}}$ to the dephasing rate. Averaging the amplitudes A_k^μ over fluctuations of $n_\mu[x(t)]$ that occur on the time scale of Γ^{-1}, we find $\gamma_\varphi^{\text{p}} \sim \sim \alpha^2\Gamma T/\Delta$. It follows that for $\gamma \ll \alpha \ll 1$ the dephasing due to the non-Gaussian zero-mode fluctuations of $J(t)$ is much stronger than that induced by plasmons.

4. Disordered noninteracting ring. In the above calculations we considered the case of the clean interacting ring. Now we neglect interaction and discuss the effect of disorder on the high-temperature conductance of the ring.

4.1. Long-range disorder. One of the realizations of the disorder is a weak smooth random potential with the correlation length much exceeding the electron Fermi wavelength. In this case, backscattering by disorder is exponentially suppressed, so that the potential only leads to the additional phase shift between the right and left-moving electron waves propagating from contact a to contact b along upper and lower shoulder of interferometer, respectively (with zero winding number). We denote the disorder-induced phase difference between these two waves as $\Psi(\epsilon)$. Such an interferometer is evidently equivalent to the clean one having two arms with the lengths $(L-a)/2$ and $(L+a)/2$, where $a \approx \Psi(\epsilon_{\text{F}})/k_{\text{F}}$. Then, from Eq. (13) we find

$$\mathcal{T}(\phi) = 2\gamma\big\{F[\sin(\pi\phi), \sin(\Psi/2)] +$$
$$+ F[\cos(\pi\phi), \cos(\Psi/2)]\big\},$$

where $F(x,y) = x^2y^2/(x^2+\gamma^2y^2)$. This equation is valid provided that $T\,(d\Psi/d\epsilon)_{\epsilon=\epsilon_{\text{F}}} \ll 1$. As seen, for $\Psi \neq 0$ there are two dips in the conductance (at $\phi = 1/2$ and 0), the widths and the depths of the dips being oscillating functions of $\Psi = \Psi(\epsilon_{\text{F}})$ (in particular, $\mathcal{T}(0) = 2\gamma\cos^2(\Psi/2)$, $\mathcal{T}(1/2) = 2\gamma\sin^2(\Psi/2)$). Hence, long-range disorder leads to appearance of the additional antiresonance in the conductance at $\phi = 0$ and modifies the antiresonance near $\phi = 1/2$.

4.2. Short-range disorder. Another realization of disorder is the potential created by weak short-range impurities, randomly distributed along the ring with the concentration n_i. Let us characterize the strength of disorder by the scattering rate in the infinite wire calculated by the golden rule. For short-range potential, transport and quantum scattering rates coincide and are given by $1/\tau = 2|r|^2 v n_i$, where r is the reflection amplitude for a single impurity ($|r| \ll 1$). Substituting in this equation $n_i = N/L$ (here N is the number of impurities in the ring) we get

$$\frac{1}{\tau} = \frac{N|r|^2\Delta}{\pi\hbar}. \qquad (28)$$

We restrict ourselves to discussion of the ballistic case, $v\tau \gg L$, or, equivalently, $N|r|^2 \ll 1$.

We will see that the main effect of the short-range potential is the broadening of the antiresonances. One could expect that scattering by disorder leads to essential increase of the resonance width, when τ becomes shorter than lifetime of the electron in the ring, $\hbar/\Gamma$, which implies $N|r|^2 \gg \gamma$. Another expectation is that in the regime $N|r|^2 \gg \gamma$, when electron experiences many scatterings during the lifetime and therefore acquires random phase, the interference is suppressed, and, consequently, the depth of the dip essentially decreases. However, we will show that the scattering on the impurities comes into play at much smaller disorder strength when $N|r|^2 \sim \gamma^2$, so that for $\gamma^2 \ll N|r|^2 \ll 1$ the dip is essentially broadened. Also, in contrast to the naive expectation, its depth remains on the order of γ.

Now we modify the matrix $\hat{A}$, taking into account the scattering on the impurities. This matrix becomes complicated, since it includes the amplitudes of all the trajectories with scatterings on both contacts and impurities, after which an electron returns to contact b.

However, in the case $\delta\phi \ll 1$, $\gamma \ll 1$, and $N|r|^2 \ll 1$, $\hat{A}$ can be simplified [40]:

$$\hat{A} \approx (1-2\gamma)e^{i\beta}\begin{bmatrix} \sqrt{1-|R|^2}e^{-2i\pi\phi} & R \\ -R^* & \sqrt{1-|R|^2}e^{2i\pi\phi} \end{bmatrix}.$$

Here, β is the small forward scattering phase for a complex scatterer consisting of N impurities. This phase is added to the geometrical phase kL and, therefore, drops out after thermal averaging. The off-diagonal element, R, is, up to a phase factor, the reflection amplitude from a complex of N impurities. One can expand R with respect to r. In the lowest order in r we obtain $R \approx r\sum_{\nu=1}^{N} e^{-2ikx_\nu}$. This expression takes into account only one backscattering on impurities during a revolution around the ring, and is valid in the case $N|r|^2 \ll 1$. We see that R depends on positions of all impurities in the ring $R = R(x_1, \ldots, x_N)$.

Let us now assume that impurities are randomly distributed along the ring. This allows us to use Eq. (7) while performing averaging over k. The sum in Eq. (7) can be calculated exactly [40]. One can use Eq. (A5) of Ref. [40] which simplifies after expansion of the numerator and denominator with respect to γ, r and $\delta\phi$. Calculations yield the following expression for the transmission coefficient:

$$\mathcal{T} \approx 2\gamma\left\langle \frac{\pi^2\delta\phi^2 + (\mathrm{Im}R)^2/4}{\pi^2\delta\phi^2 + \gamma^2 + |R|^2/4}\right\rangle_\epsilon. \qquad (29)$$

This equation is valid provided that $\gamma \ll 1$, $N|r|^2 \ll 1$, and $\delta\phi \ll 1$. The relation between $\sqrt{N}|r|$ and γ can be arbitrary. Physically, appearance of terms proportional to $(\mathrm{Im}R)^2$ and $|R|^2$ in the numerator and denominator of Eq. (29), respectively, is due to the disorder-induced repulsion in the pairs of close levels in the ring Ref. [40].

In order to perform the averaging over k, we notice, that for random impurity distribution the averaging over k is equivalent to averaging over x_ν: $\langle\cdots\rangle_k = \langle\cdots\rangle_{x_1\cdots x_N}$. Here, we present result for $N \gg 1$:

$$\mathcal{T} \approx \frac{2\gamma}{s^2}\int_0^\infty dx \frac{\pi^2\delta\phi^2(1+x) + s^2/2}{(1+x)^2}\exp\left(-x\frac{\pi^2\delta\phi^2+\gamma^2}{s^2}\right), \qquad (30)$$

where $s^2 = N|r|^2/4$ (more detailed discussion can be found in Ref. [40]). This dependence is plotted in Fig. 6. We see that the transmission coefficient at $\phi = 1/2$ is no longer equal to zero and the antiresonance broadens. It is also notable that the dip has a non-Lorentzian shape.

Let us discuss two limiting cases. For $\sqrt{N}|r| \ll \gamma$, the minimal value of conductance is given by $\mathcal{T}|_{\delta\phi=0} \approx \approx N|r|^2/4\gamma$, and the width of the antiresonances increases from γ to $\gamma' = \gamma + \delta$ where $\delta \sim N|r|^2/\gamma$. The

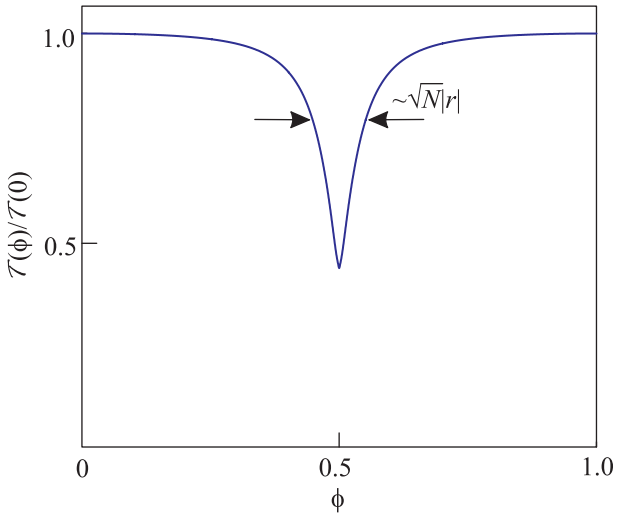

Fig. 6. Antiresonance in high-temperature transmission coefficient in the presence of N randomly distributed impurities for $\sqrt{N}|r| \gg \gamma$

relative contribution of the disorder to the resonance width, $\delta/\gamma \sim N|r|^2/\gamma^2 = \hbar/\gamma\Gamma\tau$, is enhanced by a factor $\gamma^{-1} \gg 1$ in comparison with naive expectation $\hbar/\Gamma\tau$. In the opposite limiting case, $\sqrt{N}|r| \gg \gamma$, we get $\mathcal{T}|_{\delta\phi=0} \approx \gamma$, so that the depth of the antiresonance is two times smaller compared with the case of clean ring, while the width is given by $\gamma' \sim \sqrt{N}|r|$.

5. Non-interacting ring with spin-orbit coupling. The effect of the spin-orbit (SO) interaction on the properties of one-dimensional (1D) and quasi one-dimensional systems, in particular 1D quantum wires and rings, has attracted much attention [52–73]. The rotation of electron spin in the built-in SO magnetic field results in a spin phase shift between clockwise and counterclockwise waves, which is a manifestation of the AC effect [73, 74]. The AC phase is the spin analog of the orbital AB phase. More precisely, the AC phase is additional with respect to AB phase and exists even at zero external magnetic field ($\Phi = 0$). An important consequence is the existence of the AC oscillations of zero-field conductance $G(0)$ with the strength of the SO coupling. The AC oscillations were intensively discussed theoretically [52–58, 61–64, 66–70, 72] and their signatures were observed experimentally [59, 60]. Another consequence, especially important from the point of view of possible applications, is that the unpolarized incoming electron beam acquires polarization after passing through the ring, so that the ring may serve as a spin polarizer. The latter effect was recently discussed in a number of publications [55–57, 61, 63, 64, 66, 69, 70] mostly concerned with the study of the zero-temperature case. The finite tempera-

ture effects were also analyzed on the basis of numerical simulations [57, 63, 69].

In this section, we address the role of SO coupling in the transport through a single-channel ring of radius R. We assume that the SO interaction is described by the Rashba Hamiltonian, which for the case of a straight wire reads $\hat{H}_{\rm SO} = \alpha[\mathbf{n}\times\hat{\boldsymbol{\sigma}}]\,\mathbf{p}$. Here $\mathbf{n}$ is the unit vector parallel to built-in electric field, $\hat{\boldsymbol{\sigma}}$ is the vector of the Pauli matrices, α is the constant of the SO interaction, and $\mathbf{p} = \hbar\mathbf{k}$ is the electron momentum. In a curved wire, $\mathbf{n}$ depends on the coordinate, and the Hamiltonian becomes [53, 54] $\hat{H}_{\rm SO} = (\alpha/2)\{[\mathbf{n}\times\hat{\boldsymbol{\sigma}}],\mathbf{p}\}$, where $\{\ldots\}$ stands for the anticommutator. For a ring with axially symmetric built-in field, $\mathbf{n} = (\cos\varphi\cos\theta, \sin\varphi\cos\theta, \sin\theta)$, we find

$$\hat{H}_{\rm SO} = \frac{i\alpha\hbar}{2R}\left\{\begin{bmatrix}\cos\theta & -\sin\theta e^{-i\varphi}\\ -\sin\theta e^{i\varphi} & -\cos\theta\end{bmatrix}, D_\varphi\right\}. \quad (31)$$

Here, $D_\varphi = \partial/\partial\varphi + i\phi$, φ is the angle coordinate of the electron in the ring, θ is the angle between effective SO-induced magnetic field $\mathbf{B}_{\rm eff}$ (this field is proportional to $\alpha[\mathbf{p}\times\mathbf{n}]$) and the z axis. The problem can be treated quasiclassically assuming that $kR \gg 1$ and $\alpha \ll v$. Within this approximation the effect of the SO interaction is fully described by the rotation of the electron spin in the field $\mathbf{B}_{\rm eff}$, which varies along the electron trajectory [53, 54].

The sum of the amplitudes of the trajectories having length L_n, initial spin state $|\chi_i\rangle$, and final spin state $|\chi_f\rangle$ is given by $\langle\chi_f|\hat{\beta}_n|\chi_i\rangle$, where $\hat{\beta}_n$ are now 2×2 matrices. The amplitude of transmission through the ring with spin state changing from $|\chi_i\rangle$ to $|\chi_f\rangle$ is given by $\langle\chi_i|\hat{t}|\chi_f\rangle$, where $\hat{t} = \hat{t}(\phi,\epsilon) = \sum_{n=0}^{\infty}\hat{\beta}_n\exp(ikL_n)$. The transmission coefficient reads

$$\mathcal{T} = \frac{1}{2}\big\langle{\rm Tr}\;\hat{t}\,\hat{t}^\dagger\big\rangle_\epsilon = \frac{1}{2}{\rm Tr}\;\hat{\mathcal{T}}, \quad \hat{\mathcal{T}} = \sum_{n=0}^{\infty}\hat{\beta}_n\hat{\beta}_n^\dagger. \quad (32)$$

The electrons passing through the ring acquire spin polarization. For the case of unpolarized incoming electron beam the spin polarization is calculated as

$$\mathbf{P} = \frac{\big\langle{\rm Tr}\;\hat{\boldsymbol{\sigma}}\hat{t}\hat{t}^\dagger\big\rangle_\epsilon}{2\mathcal{T}} = \frac{{\rm Tr}\;\hat{\boldsymbol{\sigma}}\hat{\mathcal{T}}}{2\mathcal{T}}, \quad (33)$$

and, therefore, is also expressed in terms of $\hat{\beta}_n$.

The matrix $\hat{A}$ becomes a block matrix:

$$\hat{A} = \begin{bmatrix} t_{in}^2 e^{-2\pi i\phi}\hat{M} + t_b^2 & t_b t_{in}(e^{-2\pi i\phi}\hat{M}+1)\\ t_b t_{in}(e^{2\pi i\phi}\hat{M}^{-1}+1) & t_{in}^2 e^{2\pi i\phi}\hat{M}^{-1} + t_b^2\end{bmatrix}.$$

The matrix $\hat{M}$ ($\hat{M}^{-1}$) describes spin rotation after passing a full circle starting from contact b and propagating in counterclockwise (clockwise) direction. It can be written as $\hat{M} = \exp(-i\boldsymbol{\rho}\hat{\boldsymbol{\sigma}}/2)$, where $\boldsymbol{\rho}$ is the vector of spin rotation for counterclockwise propagation around the ring (starting from contact b): $\boldsymbol{\rho} = 4\pi\delta(\boldsymbol{e}_x\sin\vartheta - \boldsymbol{e}_z\cos\vartheta)$, where

$$\delta = \sqrt{\frac{1}{4} + \xi\cos\theta + \xi^2} - \frac{1}{2},\ \tan\vartheta = \frac{\xi\sin\theta}{1/2 + \xi\cos\theta}. \quad (34)$$

The coefficient $\xi = \alpha kR/\hbar v$ is the dimensionless parameter characterizing the strength of SO interaction. Physically, ξ is the angle of spin rotation in the local field $\mathbf{B}_{\rm eff}$ during the time on the order of R/v. In the simplest case $\theta = 0$, ξ is proportional to the angle of the spin rotation after passing around the ring.

The eigenvectors of $\hat{M}$ are the spinors $\chi^\uparrow$ and $\chi^\downarrow$ corresponding to spin orientation along $\boldsymbol{\rho}$ and $-\boldsymbol{\rho}$: $\hat{M}\chi^\uparrow = \exp(-i\cdot 2\pi|\delta|)\chi^\uparrow$, $\hat{M}\chi^\downarrow = \exp(i\cdot 2\pi|\delta|)\chi^\downarrow$. As follows from these equations, $2\pi|\delta|$ is the AC phase [73, 74] induced by the SO interaction.

For $\xi \gg 1$, the frequency of spin precession in the field $\mathbf{B}_{\rm eff}$ is much larger than the orbital frequency v/R and the direction of the spin follows adiabatically the direction of $\mathbf{B}_{\rm eff}$. In this case, $2\pi\delta \approx 2\pi\xi - \pi(1-\cos\theta)$. Thus, in the adiabatic limit the AC phase separates into two parts [53]: dynamical contribution $2\pi\xi$ and geometrical SO Berry phase [75] $\pi(1-\cos\theta)$ which is the half of the solid angle subtended by $\mathbf{B}_{\rm eff}$ when electron passes the full circle.

The calculation presented in Ref. [41] yields $\hat{\mathcal{T}}(\phi) = \mathcal{T}_0(\phi-|\delta|)|\chi_\uparrow\rangle\langle\chi_\uparrow| + \mathcal{T}_0(\phi+|\delta|)|\chi_\downarrow\rangle\langle\chi_\downarrow|$, where $\mathcal{T}_0$ is the transmission coefficient of the spinless electrons given by Eq. (8). The expressions for the full transmission coefficient and the spin polarization become

$$\mathcal{T}(\phi) = \frac{\mathcal{T}_0(\phi+\delta) + \mathcal{T}_0(\phi-\delta)}{2},\ \mathbf{P}(\phi) = P(\phi)\frac{\boldsymbol{\rho}}{\rho}, \quad (35)$$

where

$$P(\phi) = \frac{\mathcal{T}_0(\phi+|\delta|) - \mathcal{T}_0(\phi-|\delta|)}{\mathcal{T}_0(\phi+|\delta|) + \mathcal{T}_0(\phi-|\delta|)}. \quad (36)$$

These equations are illustrated in Fig. 7. As seen, there are two dips (per period) in the function $\mathcal{T}(\phi)$, corresponding to $\phi = 1/2\pm\delta$. At these two points the incoming electrons with spin states described, respectively, by $\tilde{\chi}^\downarrow$ and $\tilde{\chi}^\uparrow$ are totally blocked by the destructive interference. Therefore, the tunneling current becomes fully polarized in the direction of $\boldsymbol{\rho}$ for $\phi = 1/2\pm\delta$.

One sees that the SO-induced splitting of the resonances is proportional to the AC phase $2\pi\delta$. Equations (35) and (36) reveal coexisting of two types of oscillations: the AB oscillations with ϕ and AC oscillations with δ. Importantly, AC oscillations of tunneling conductance exist even in the case of zero external field.

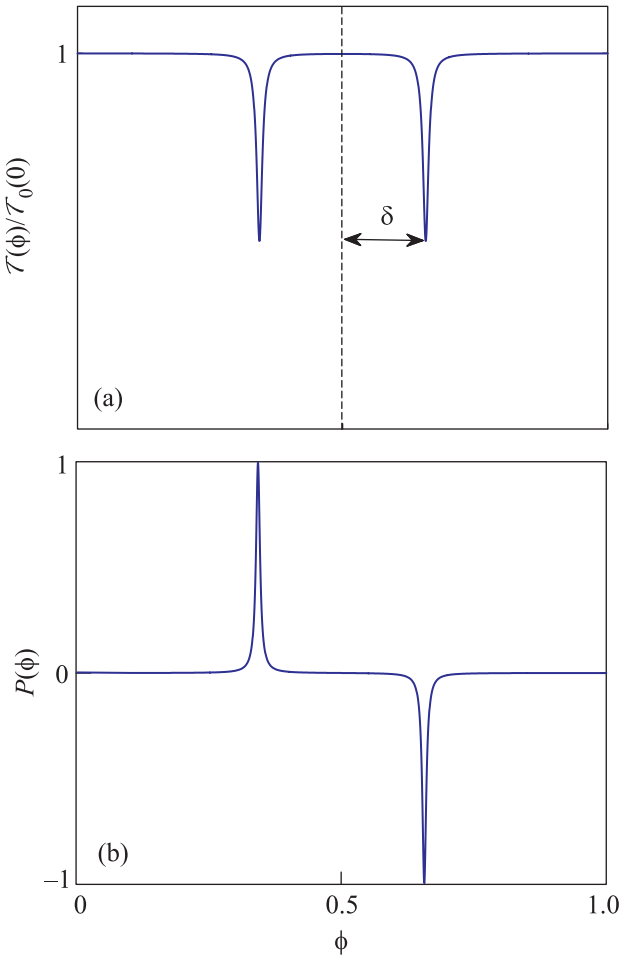

Fig. 7. Transmission coefficient (a) and the spin polarization of the transmitted electrons (b) in the direction of vector $\boldsymbol{\rho}$ for the ring with the SO interaction ($\gamma = 0.02$, $\xi = 0.2$, $\theta = \pi/4$)

Indeed, for $\phi = 0$, since $\mathcal{T}_0(\delta)$ is an even function, one finds $\mathcal{T} = \mathcal{T}_0(\delta)$, $P = 0$. Thus, the transmission coefficient exhibits the AC oscillations with the period $\delta = 1$. For the case of an almost closed ring, $\gamma \ll 1$, the oscillations have the form of sharp antiresonances periodic in δ.

Equations presented in this section are valid for $T \gg \Delta$ and arbitrary strength of tunneling coupling ($0 < \gamma < \infty$). They represent a generalization of the analytical results obtained previously [55, 57, 58, 61, 63] for $T = 0$ and strong tunneling coupling ($\gamma \simeq 1$).

6. Summary. In this review, we have addressed the Aharonov–Bohm effect in transport through a single-channel quantum ring tunnel-coupled to the leads, focusing on the case of large temperature (compared to the level spacing). Remarkably, in this high-temperature regime, there are quantum interference effects that survive thermal averaging. In a clean non-interacting ring (Section 2), the tunneling conductance exhibits sharp dips at half-integer values of the magnetic flux. The conductance vanishes exactly at these values because of destructive interference of amplitudes of tunneling through degenerate energy levels of the ring. This effect is not affected by thermal averaging.

Electron-electron interactions lead to profound and unusual effects in transport through a single-channel ring (Section 3), owing to an interplay of the AB effect and quantization in an almost close system. The quantization of the circular current inside the ring gives rise to the phenomenon of Persistent-Current Blockade. The tunneling conductance through the ring, $G(\phi)$, exhibits a series of sharp antiresonances broadened by dephasing, the distance between which is controlled by the interaction strength. The dominant contribution to the dephasing rate is due to tunneling-induced fluctuations of the circular current – we have termed this novel type of dephasing "Zero-Mode dephasing". Importantly, the quantization of excitation spectra in an almost closed geometry significantly suppresses dephasing, as compared to setups with open geometry.

In Section 4 we addressed the effect of weak disorder on the high-temperature transport through a ring. In the absence of interaction, the short-range disorder potential broadens the AB antiresonances, while the long-range smooth potential leads to appearing of negative resonant peaks at integer values of the flux.

The role of the spin-orbit coupling was discussed in Section 5, where the high-temperature transmission coefficient $\mathcal{T}(\phi)$ and the spin polarization $\mathbf{P}(\phi)$ were considered in the presence of the Rashba SO interaction. Both $\mathcal{T}(\phi)$ and $\mathbf{P}(\phi)$ reveal coexistence of two types of periodic oscillations: the AB oscillations with magnetic flux and the Aharonov–Casher oscillations with the strength of SO interaction. For weak tunneling coupling, the oscillations have the form of the sharp antiresonances. Specifically, there are two antiresonances (per period) in the dependence $\mathcal{T}(\phi)$ (instead of one antiresonance without SO coupling). In the vicinity of each antiresonance, the electron beam passing through the ring acquires strong spin polarization.

We thank D.N. Aristov, Y. Gefen, and P. Wölfle for valuable discussions. The work was supported by Russian Foundation for Basic Research, by programs of the Russian Academy of Sciences, and the EU Network Grant InterNoM.

1. Yu. V. Nazarov and Ya. M. Blanter, *Quantum Transport: Introduction to Nanoscience*, Cambridge University Press, Cambridge (2009).

2. Y. Aharonov and D. Bohm, Phys. Rev. B **115**, 485 (1959).
3. A. G. Aronov and Yu. V. Sharvin, Rev. Mod. Phys. **59**, 755 (1987).
4. A. G. Aronov and Yu. V. Sharvin, Rev. Mod. Phys. **59**, 755 (1987).
5. A. Yacoby, M. Heiblum, D. Mahalu, and H. Shtrikman, Phys. Rev. Lett. **74**, 4047 (1995).
6. A. Yacoby, R. Schuster, and M. Heiblum, Phys. Rev. B **53**, 9583 (1996)
7. A. van Oudenaarden, M. H. Devoret, Yu. V. Nazarov, and J. E. Mooij, Nature **391**, 768 (1998).
8. A. A. Bykov, A. K. Bakarov, L. V. Litvin, and A. I. Toropov, JETP Lett. **72**, 209 (2000).
9. A. A. Bykov, D. G. Baksheev, L. V. Litvin, V. P. Migal, E. B. Olshanetskii, M. Casse', D. K. Maude, and J. C. Portal, JETP Lett. **71**, 434 (2000).
10. O. M. Auslaender, A. Yacoby, R. de Picciotto, K. W. Baldwin, L. N. Pfeiffer, and K. W. West, Science **295**, 825 (2002).
11. Y. Ji, Y. Chung, D. Sprinzak, M. Heiblum, D. Mahalu, and H. Shtrikman, Nature **422**, 415 (2003).
12. P. Samuelsson, E. V. Sukhorukov, and M. Buttiker, Phys. Rev. Lett. **92**, 026805 (2004).
13. M. Avinun-Kalish, M. Heiblum, O. Zarchin, D. Mahalu, and V. Umansky, Nature **436**, 529 (2005).
14. I. Neder, M. Heiblum, Y. Levinson, D. Mahalu, and V. Umansky, Phys. Rev. Lett. **96**, 016804 (2006).
15. I. Neder, N. Ofek, Y. Chung, M. Heiblum, D. Mahalu, and V. Umansky, Nature **448**, 333 (2007).
16. I. Neder, M. Heiblum, D. Mahalu, and V. Umansky, Phys. Rev. Lett. **98**, 036803 (2007).
17. P. Roulleau, F. Portier, D. C. Glattli, P. Roche, A. Cavanna, G. Faini, U. Gennser, and D. Mailly, Phys. Rev. B **76**, 161309 (2007).
18. P. Roulleau, F. Portier, and P. Roche, Phys. Rev. Lett. **100**, 126802 (2008).
19. Y. Zhang, D. T. McClure, E. M. Levenson-Falk, C. M. Marcus, L. N. Pfeiffer, and K. W. West, Phys. Rev. B **79**, 241304 (2009).
20. E. Weisz, H. K. Choi, M. Heiblum, Y. Gefen, V. Umansky, and D. Mahalu, Phys. Rev. Lett. **109**, 250401 (2012).
21. H. R. Shea, R. Martel, and Ph. Avouris, Phys. Rev. Lett. **84**, 4441 (2000).
22. S. Zou, D. Maspoch, Y. Wang, C. A. Mirkin, and G. C. Schatz, Nano Lett. **7**, 276 (2007).
23. V. Piazza, F. Beltram, W. Wegscheider, C. T. Liang, and M. Pepper, Phys. Rev. B **62**, 10630(R) (2000).
24. A. Fuhrer, S. Lüscher, T. Ihn, T. Heinzel, K. Ensslin, W. Wegscheider, and M. Bichler, Nature **413**, 822 (2001).
25. U. F. Keyser, C. Fühner, S. Borck, R. J. Haug, M. Bichler, G. Abstreiter, and W. Wegschreider, Phys. Rev. Lett. **90**, 196691 (2003).
26. M. Büttiker, Y. Imry, and M. Ya. Azbel, Phys. Rev. A **30**, 1982 (1984).
27. Y. Gefen, Y. Imry, and M. Ya. Azbel, Phys. Rev. Lett. **52**, 129 (1984).
28. M. Büttiker, Y. Imry, R. Landauer, and S. Pinhas, Phys. Rev. B **31**, 6207 (1985).
29. M. V. Moskalets, Low Temp. Phys. **23**, 824 (1997).
30. Q. Li and C. M. Soukoulis, Phys. Rev. B **33**, 7318 (1986).
31. J. M. Mao, Y. Huang, and J. M. Zhou, J. Appl. Phys. **73**, 1853 (1993).
32. E. P. Nakhmedov, H. Feldmann, and R. Oppermann, Eur. Phys. J. B **16**, 515 (2000).
33. M. A. Kokoreva, V. A. Margulis, and M. A. Pyataev, Physica E **43**, 1610 (2011).
34. J. M. Kinaret, M. Jonson, R. I. Shekhter, and S. Eggert, Phys. Rev. B **57**, 3777 (1998).
35. M. Eroms, L. Mayrhofer, and M. Grifoni, Phys. Rev. B **78**, 075403 (2008).
36. Y. Gefen, Y. Imry, and M. Ya. Azbel, Surface Science **142**, 203 (1984).
37. E. A. Jagla and C. A. Balseiro, Phys. Rev. Lett. **70**, 639 (1993).
38. A. P. Dmitriev, I. V. Gornyi, V. Yu. Kachorovskii, and D. G. Polyakov, Phys. Rev. Lett. **105**, 036402 (2010).
39. T. Giamarchi, *Quantum Physics in One Dimension*, Oxford University Press, Oxford (2004).
40. P. M. Shmakov, A. P. Dmitriev, and V. Yu. Kachorovskii, Phys. Rev. B **87**, 235417 (2013).
41. P. M. Shmakov, A. P. Dmitriev, and V. Yu. Kachorovskii, Phys. Rev. B **85**, 075422 (2012).
42. K. Le Hur, Phys. Rev. B **65**, 233314 (2002).
43. K. Le Hur, Phys. Rev. Lett. **95**, 076801 (2005).
44. K. Le Hur, Phys. Rev. B **74**, 165104 (2006).
45. I. V. Gornyi, A. D. Mirlin, and D. G. Polyakov, Phys. Rev. Lett. **95**, 046404 (2005).
46. I. V. Gornyi, A. D. Mirlin, and D. G. Polyakov, Phys. Rev. B **75**, 085421 (2007).
47. D. N. Aristov, A. P. Dmitriev, I. V. Gornyi, V. Yu. Kachorovskii, D. G. Polyakov, and P. Wölfle, Phys. Rev. Lett. **105**, 266404 (2010).
48. F. D. M. Haldane, J. Phys. C **14**, 2585 (1981).
49. Y. M. Galperin, B. L. Altshuler, J. Bergli, and D. V. Shantsev, Phys. Rev. Lett. **96**, 097009 (2006).
50. J. Schriefl, Y. Makhlin, A. Shnirman, and G. Schön, New J. Phys. **8**, 1 (2006).
51. C. Neuenhahn, B. Kubala, B. Abel, and F. Marquardt, Phys. Stat. Sol. b **246**, 1018 (2009).
52. H. Mathur and A. D. Stone, Phys. Rev. B **44**, 10957 (1991).
53. A. G. Aronov and Y. B. Lyanda-Geller, Phys. Rev. Lett **70**, 343 (1993).
54. T. Z. Qian and Z. B. Su, Phys. Rev. Lett. **72**, 2311 (1994).

55. J. Nitta, F. E. Meijer, and H. Takayanji, Appl. Phys. Lett **75**, 695 (1999).
56. D. Frustaglia and K. Richter, Phys. Rev. B **69**, 235310 (2004).
57. B. Molnar, F. M. Peeters, and P. Vasilopoulos, Phys. Rev. B **69**, 155335 (2004).
58. U. Aeberland, K. Wakabayashi, and M. Sigrist, Phys. Rev. B **72**, 075328 (2005).
59. M. Konig, A. Tschetschetkin, E. M. Hankiewicz, J. Sinova, V. Hock, V. Daumer, M. Schafer, C. R. Becker, H. Buhmann, and L.W. Molenkamp, Phys. Rev. Lett. **96**, 076804 (2006).
60. T. Bergsten, T. Kobayashi, Y. Sekine, and J. Nitta, Phys. Rev. Lett. **97**, 196803 (2006).
61. R. Citro and F. Romeo, Phys. Rev. B **73**, 233304 (2006).
62. M. Pletyukhov, V. Gritsev, and N. Pauget, Phys. Rev. B **74**, 045301 (2006).
63. R. Citro and F. Romeo, Phys. Rev. B **74**, 115329 (2006).
64. A. A. Kovalev, M. F. Borunda, T. Jungwirth, L. W. Molenkamp, and J. Sinova, Phys. Rev. B **76**, 125307 (2007).
65. F. Cheng and G. Zhou, J. Phys.: Condens. Matter **19**, 136215 (2007).
66. F. Romeo, R. Citro, and M. Marinaro, Phys. Rev. B **78**, 245309 (2008).
67. A. M. Lobos and A. A. Aligia, Phys. Rev. Lett. **100**, 016803 (2008).
68. M. Pletyukhov and U. Zülike, Phys. Rev. B **77**, 193304 (2008).
69. V. Moldoveanu and B. Tanatar, Phys. Rev. B **81**, 035326 (2010).
70. A. Aharony, Y. Tokura, G. Z. Cohen, O. Entin-Wohlman, and S. Katsumoto, Phys. Rev. B **84**, 035323 (2011).
71. C. X. Liu, J. C. Budisch, P. Recher, and B. Trauzettel, Phys. Rev. B **83**, 035407 (2011).
72. P. Michette and P. Recher, Phys. Rev. B **83**, 125420 (2011).
73. Y. Aharonov and A. Casher, Phys. Rev. Lett **53**, 319 (1984).
74. H. Mathur and A. D. Stone, Phys. Rev. Lett. **68**, 2964 (1992).
75. M. V. Berry, Proc. R. Soc. London A **392**, 45 (1984).